Localization of bilirubin in phospholipid bilayers by parallax analysis of fluorescence quenching[1]

Stephen D. Zucker,[2,*] Wolfram Goessling,[†] Emma J. Bootle,[†] and Coreen Sterritt[†]

Division of Digestive Diseases,* University of Cincinnati, Cincinnati, OH 45243; and Department of Medicine,† Brigham and Women's Hospital, Boston, MA 02115

ABSTRACT **It has been proposed that the neurotoxicity observed in severely jaundiced infants results from the binding of unconjugated bilirubin to nerve cell membranes. However, despite potentially important clinical ramifications, there remains significant controversy regarding the physical nature of bilirubin-membrane interactions. We used the technique of parallax analysis of fluorescence quenching (Chattopadhyay, A., and E. London. 1987. Biochemistry. 26: 39–45) to measure the depth of penetration of bilirubin in model phospholipid bilayers. The localization of unconjugated bilirubin and ditaurobilirubin within small unilamellar vesicles composed of dioleoylphosphatidylcholine was determined through an analysis of the quenching of bilirubin fluorescence by spin-labeled phospholipids, and by bilirubin-mediated quenching of a series of anthroyloxy fatty acid probes at various depths within the membrane bilayer. Findings were further verified with potassium iodide as an aqueous quencher. Our results indicate that, at pH 10, unconjugated bilirubin localizes approximately 20 Å from the bilayer center, in the region of the polar head groups. Further analyses suggest a modest influence of pH, membrane cholesterol content, and vesicle diameter on the bilirubin penetration depth. Taken together, these data support that, under physiologic conditions, bilirubin localizes to the polar region of phospholipid bilayers, near the membrane-water interface.**—Zucker, S. D., W. Goessling, E. J. Bootle, and C. Sterritt. **Localization of bilirubin in phospholipid bilayers by parallax analysis of fluorescence quenching.** ***J. Lipid Res.*** **2001.** 42: **1377–1388.**

Supplementary key words membranes • resonance energy transfer • kernicterus • cholesterol • ditaurobilirubin • quantum yield • potassium iodide • binding affinity

Unconjugated bilirubin, the main product of heme catabolism, is a tetrapyrrole composed of two rigid, planar dipyrrole units joined by a methylene bridge (1). The predominant physiologic isomer, bilirubin IXα, is maintained in a ridge-tile conformation by intramolecular hydrogen bonding between the two carboxylic acid groups and the opposing dipyrromethenone moieties. Bilirubin is unusual in that it exhibits limited aqueous solubility at physiologic pH (2) and yet also is poorly soluble in apolar solvents (3). The physical characteristics of the bilirubin molecule that result in its distinctive solubility may have important physiological ramifications. For example, it is postulated that the potentially severe neurotoxicity associated with neonatal hyperbilirubinemia results from the interaction of bilirubin with neuronal membranes (4–6).

Although the affinity of bilirubin for phospholipids has been well documented (3, 7, 8), the nature of this interaction is poorly understood. It has been concluded from equilibrium binding studies that bilirubin partitions into elements of free volume within the hydrophobic core of phospholipid bilayers (9). This hypothesis is supported by high pressure infrared spectroscopic analyses of vesicles composed of dimyristoylphosphatidylcholine and dioleoylphosphatidylcholine, which indicate that bilirubin localizes to the polymethylene chain region between the carbonyl carbon and the methylene group two carbons from the methyl terminus (10). In contrast, other investigators have argued that the poor solubility of bilirubin in apolar solvents mitigates against intercalation within the phospholipid acyl chains (11, 12). Support for the localization of bilirubin in the region of the phospholipid polar head groups is derived from air-water interface studies (13) and from resonance Raman spectroscopic analyses of the interaction of bilirubin IXα with sphingomyelin liposomes (14). Furthermore, the free energy of activation (15, 16) and the rate of solvation (15, 17) of bilirubin from lipid vesicles are lower than for medium- or long-chain fatty acids (18–20), suggesting that penetration of bilirubin into the hydrophobic membrane core is limited (15). A unifying hypothesis, based on calorimetric and ^{1}H nuclear magnetic resonance analyses, holds that bilirubin localizes either to the apolar or to the polar region of phospholipid bilayers depending on the ionization state of the molecule (21).

In an attempt to resolve these conflicting data, we used the method of parallax analysis of fluorescence quenching,

Abbreviations: 2-, 6-, 9-, or 12-AS, 2-, 6-, 9-, or 12-(9-anthroyloxy)-stearic acid; BDT, ditaurobilirubin; DOPC, 1,2-dioleoyl-*sn*-glycero-3-phosphocholine (dioleoylphosphatidylcholine); LUV, large unilamellar vesicles; 5- or 12-SLPC, 1-palmitoyl-2-(5- or 12-doxyl)stearoyl-*sn*-glycero-3-phosphocholine; SUV, small unilamellar vesicles.

[1] Preliminary reports of this work have been published in abstract form (Zucker, S. D., and E. J. Bootle. 1996. *Hepatology.* **24:** 604A; and Zucker, S. D., and W. Goessling. 2000. *Hepatology.* **32:** 427A).

[2] To whom correspondence should be addressed.
e-mail: zuckersd@email.uc.edu

Downloaded from www.jlr.org by guest, on June 14, 2012

originally described by Chattopadhyay and London (22), to more precisely define the location of bilirubin within model phospholipid bilayers. This technique, which involves the incorporation of lipid probes labeled at varying positions along the acyl chain into membrane vesicles, previously has been used to measure the depth of penetration of a variety of fluorescent lipophilic compounds in phospholipid bilayers, with a resolution approaching 1 Å (23–25). The findings of our studies suggest that unconjugated bilirubin is associated at the polar head group region of model membranes.

EXPERIMENTAL PROCEDURES

Materials

Bilirubin (unconjugated bilirubin) and ditaurobilirubin (bilirubin conjugate-ditaurate·2Na; BDT) were obtained from Porphyrin Products (Logan, UT). Bilirubin was further purified according to the method of McDonagh and Assisi (26). Dioleoylphosphatidylcholine (1,2-dioleoyl-*sn*-glycero-3-phosphocholine) and spin-labeled phosphatidylcholines, 1-palmitoyl-2-(5-doxyl)-stearoyl-*sn*-glycero-3-phosphocholine (5-SLPC) and 1-palmitoyl-2-(12-doxyl)stearoyl-*sn*-glycero-3-phosphocholine (12-SLPC), were purchased from Avanti Polar Lipids (Birmingham, AL). A series of stearic acid probes labeled at the 2-, 6-, 9-, or 12-position with a 9-anthroyloxy group (2-, 6-, 9-, or 12-AS) were purchased from Molecular Probes (Eugene, OR). Cholesterol was obtained from Nu-Chek Prep (Elysian, MN).

Preparation of unilamellar phospholipid vesicles

Vesicles composed of dioleoylphosphatidylcholine (DOPC) were used in our analyses because the localization of the spin-labeled phospholipid and anthroyloxy-labeled stearic acid probes utilized in the measurement of bilirubin penetration depth have been precisely defined in DOPC membranes (22, 24, 27). Small unilamellar vesicles (SUV) were prepared by sonication, according to the method of DiCorleto and Zilversmit (28). A chloroform solution of DOPC was evaporated to dryness under argon, solubilized in ether, and then re-evaporated to form a uniform film. Phospholipids were desiccated overnight under vacuum and resuspended in 0.1 M potassium phosphate solution buffered at pH 10, unless otherwise indicated. The lipid suspension was sonicated under argon atmosphere in a bath sonicator (Laboratory Supplies Company, Hicksville, NY) until clear. Cholesterol and/or fluorescently labeled probes were incorporated into vesicles by adding the lipids, at specified molar ratios, to the chloroform solution of DOPC before desiccation. Large unilamellar vesicles (LUV) were prepared by the injection method of Kremer et al. (29), as previously described (17). Briefly, phospholipids were desiccated, resuspended in ethanol, and slowly injected into a stirred solution of 0.1 M potassium phosphate, using a tuberculin syringe fitted with a 22-gauge blunt needle. The resultant lipid vesicles were exhaustively dialyzed to remove retained ethanol, and phospholipid concentrations were quantified by the lipid phosphorus assay method of Bartlett (30). The mean hydrodynamic diameter of the vesicle preparations was determined by quasielastic light scattering (15, 31).

Measurement of bilirubin penetration depth with spin-labeled phospholipid probes

The depth of bilirubin penetration into phospholipid vesicles composed of DOPC was determined by parallax analysis of fluorescence quenching. In the original reports of this technique (22, 23), precise localization of fluorescent lipid probes within DOPC vesicles was achieved by examining the quenching of probe fluorescence intensity by a series of spin-labeled phospholipids located at defined depths within the bilayer. As bilirubin exhibits intrinsic fluorescence when bound to membranes (32), we utilized a similar approach to determine the penetration depth of bilirubin in DOPC bilayers. Vesicles were prepared by sonicating DOPC in the presence of varying molar ratios of a phosphatidylcholine probe possessing a doxyl spin label at either the 5- or 12-position of the acyl chain (5- or 12-SLPC). Bilirubin was added to the vesicle suspension (3 ml) in a 10 × 10 mm stirred quartz cuvette to produce a final concentration of 2 μM, and steady state bilirubin fluorescence intensity (excitation, 467 nm; emission, 525 nm) was recorded with an Aminco-Bowman II fluorescence spectrophotometer maintained at 25°C with a circulating water bath. Fluorescence readings were obtained by briefly opening the excitation slit and recording the average intensity over 3 s, thereby minimizing the exposure of the sample to incident light. This approach to sample handling resulted in trivial (≤2%) loss of pigment to photo-oxidation, as assessed by absorption spectroscopy. Readings were routinely corrected for light-scattering background. Experiments were conducted at a phospholipid concentration of 0.2 mM, although similar results were obtained when using vesicle concentrations ranging from 0.1 to 1.0 mM phospholipid.

Incorporation of bilirubin into DOPC vesicles was accomplished by dissolving the bile pigment in alkaline (pH 12.0) potassium phosphate, as previously described (15, 33). The addition of a small aliquot (≤1%, v/v) of the bilirubin solution to a suspension of vesicles buffered in 0.1 M potassium phosphate was found to cause no detectable alteration in pH. Where indicated, bilirubin also was incorporated at the time of vesicle preparation by codissolving the pigment with DOPC and subjecting the mixture to sonication. All steps were performed in dim light. Vesicles were equilibrated with bilirubin at 25°C for 5 to 10 min before measuring fluorescence intensity, over which time no significant change in the bilirubin absorbance spectrum was observed. Because of the high affinity of bilirubin for membranes (8, 9) and the extremely low fluorescence quantum yield of free (aqueous) bilirubin compared with that of membrane-bound bilirubin (34), the contribution of unbound bilirubin to the overall fluorescence signal was negligible.

Because accurate localization of spin-labeled phosphatidylcholine probes within DOPC bilayers previously has been established (22), the average distance from the center of the bilayer to the bilirubin molecule (z_{cB}) can be calculated by equation 1 (22),

$$z_{cB} = \left[\frac{\left(\frac{-1}{\pi C}\right)\ln\left(\frac{F_1}{F_2}\right) - L_{21}^2}{2L_{21}}\right] + z_{c1} \qquad \textit{Eq. 1)}$$

where C is the concentration of quencher lipid per unit area, F_1 is the fluorescence intensity of bilirubin in the presence of vesicles containing the shallow quencher (5-SLPC), F_2 reflects the bilirubin fluorescence intensity in the presence of vesicles containing an equivalent mole fraction of the deep quencher (12-SLPC), L_{21} is the difference in depth between the shallow and deep quenchers, and z_{c1} is the distance from the bilayer center to the shallow quencher. Values for C were calculated by dividing the mole fraction of quencher lipid in total lipid by the surface area per phospholipid (70 Å^2) (22).

Bilirubin penetration depth as determined by the quenching of anthroyloxy stearate fluorescence

The depth of bilirubin penetration into membrane bilayers also was determined by analyzing the quenching of the fluorescence intensity of a series of anthroyloxy stearic acid probes (ex-

Downloaded from www.jlr.org by guest, on June 14, 2012

citation, 360 nm; emission, 490 nm) by bilirubin (schematically depicted in Fig. 8). In these studies, the steady state fluorescence intensity of DOPC vesicles labeled with either 2-, 6-, 9-, or 12-AS (1 mol%) was measured in the presence of increasing concentrations of bilirubin, with all data corrected for light-scattering background and bilirubin inner filter effects. Because the lateral diffusion of lipids within membranes generally is slow with respect to the fluorescence lifetime of the anthroyloxy stearate probes (35), quenching can be considered to be predominantly static (36–38). By using the two-dimensional Perrin equation for static quenching, the ratio of shallow probe fluorescence intensity (F_1) to that of the deep fluorophore (F_2) can be expressed as shown in equation 2 (22):

$$\frac{F_1}{F_2} = \frac{e^{-\pi R_1^2 C + \pi L_{F1}^2 C + \pi x^2 C}}{\left(e^{-\pi R_2^2 C + \pi L_{F2}^2 C + \pi x^2 C}\right)\left(e^{-\pi R_2^2 C + \pi L_{F2t}^2 C + \pi x_{F2t}^2 C}\right)} \quad \textit{Eq. 2)}$$

where L_{F1} reflects the vertical distance from the bilirubin molecule to the shallow fluorophore and L_{F2} represents the vertical distance from bilirubin to the deep probe. The terms R_1 and R_2 reflect the critical separation distance (R_c) between bilirubin and the shallow and deep probes, respectively, where R_c is equal to the Förster distance multiplied by 1.10 (22). It previously has been shown that Förster distance values for bilirubin-albumin donor-acceptor pairs range between 31 and 32 Å (39), suggesting that R_0 for AS-bilirubin is likely to be large compared with the thickness of the DOPC vesicle hemileaflet (22). For this reason, equation 2 takes into consideration the ability of a bilirubin molecule located in one bilayer (*cis*) leaflet to also quench the fluorescence of the deeper probe located in the opposing (*trans*) leaflet, with the subscript "t" denoting fluorophore located in the *trans* leaflet of the bilayer. The minimum closest allowable lateral approach (x) between bilirubin and the fluorophore is assumed to equal zero for probes in the *trans* leaflet (22).

Values for the distance of the shallow (z_{c1}) and deep (z_{c2}) AS probes from the center of DOPC bilayers have been well established (24). Therefore, we replaced the variables L_{F1} and L_{F2} with the terms $z_{c1} - z_{cB}$ and $z_{c2} - z_{cB}$, respectively. The additional substitution of $2z_{cB} + L_{F2}$ for L_{F2t} in equation 2 produces equation 3:

$$\ln\frac{F_1}{F_2} = -\pi C\left(z_{cB}^2 + 2z_{c1}z_{cB} + 2z_{c2}^2 - z_{c1}^2 + R_1^2 - 2R_2^2\right) \quad \textit{Eq. 3)}$$

which is of the form y = mx. According to this equation, a plot of $\ln F_1/F_2$ versus C (the mole fraction of bilirubin in total lipid/70 Å^2) should produce a line with y-intercept zero. Because all other variables can be quantified, the average distance from the bilayer center to the bilirubin molecule can be derived from the slope of the plot. Alternatively, equation 4 represents the direct calculation of z_{cB} values by solving equation 3:

$$z_{cB} = -z_{c1} \pm \sqrt{\frac{-1}{\pi C}\ln\frac{F_1}{F_2} + 2z_{c1}^2 - 2z_{c2}^2 + 2R_2^2 - R_1^2} \quad \textit{Eq. 4)}$$

Using Scatchard analysis (40), the binding affinity of bilirubin for DOPC vesicles also was determined from the quenching of steady state AS fluorescence, as previously described (41).

Iodide quenching of bilirubin fluorescence

Iodide is unable to penetrate the hydrophobic membrane core and, as a result, this quencher frequently has been used to determine the accessibility of membrane-bound proteins and other compounds to the aqueous phase (42–46). We analyzed the quenching of bilirubin fluorescence by potassium iodide in an attempt to validate further the localization of bilirubin within DOPC bilayers. A concentrated stock solution (5 M) of KI was prepared in the presence of 0.1 mM $Na_2S_2O_3$ to prevent formation of I_3^- (45). Serial aliquots (3 μl) of the KI stock solution were added to a 3.0-ml suspension of DOPC vesicles (200 μM phospholipid in 0.1 M potassium phosphate, pH 10), which was preincubated for 5 min with bilirubin (5 μM) in a stirred quartz cuvette. After each KI addition, steady state fluorescence intensity was recorded over a 3-s interval. Corrections for dilution (<1% of the total volume) were routinely performed.

The fluorescence quenching data were analyzed according to the Stern-Volmer relationship (42, 43) (equation 5):

$$(F_0/F) - 1 = K_{SV}[KI] \quad \textit{Eq. 5)}$$

where F_0 is the fluorescence intensity in the absence of KI, F is the fluorescence intensity at a given potassium iodide concentration, [KI], and K_{SV} is the Stern-Volmer constant, indicative of the relative exposure of the fluorophore to the iodide probe (42). On the basis of equation 5, the slope of a plot of $(F_0/F) - 1$ versus [KI] provides a measure of K_{SV}. The bimolecular rate constant (k_q) can then be estimated from the fluorescence lifetime (τ_0), using equation 6 (45, 47):

$$k_q = \frac{K_{SV}}{\tau_0} \quad \textit{Eq. 6)}$$

Measurement of fluorescence quantum yields and Förster distances

The fluorescence quantum yield (φ) for bilirubin and for 2-, 6-, 9-, and 12-AS bound to DOPC vesicles was determined relative to quinine sulfate in 0.1 N H_2SO_4 (excitation, 352 nm; emission, 380–700 nm), using a standard value for φ of 0.7 (48). Corrections were made for wavelength-dependent lamp and photomultiplier variation (49), inner filter effects (50), and light scattering (51). Förster distance (R_0) values for AS-bilirubin donor-acceptor pairs in DOPC vesicles were determined from the overlap integral J(λ) obtained from the absorption spectrum of bilirubin and AS emission spectra, on the basis of equation 7 (52):

$$R_0 = 0.211[\kappa^2 n^{-4}\varphi_{AS}J(\lambda)]^{1/6} \quad \textit{Eq. 7)}$$

where κ^2 reflects the orientation of the transition dipoles of the donor and acceptor, n is the refractive index of the medium, and φ_{AS} represents the fluorescence quantum yield of the specific AS probe. A standard value for κ^2 of 2/3 (53) and values for n of $1.38 + 0.003z_A$, where z_A corresponds to anthroyloxy probe depth (51), were utilized in the calculations. The 2/3 value for the orientation factor is considered to represent a reasonable assumption because of the lack of rigidity of the donors and acceptors, and because bilirubin possesses two orthogonally oriented transition dipoles (53–55).

Determination of energy transfer efficiencies

Energy-transfer efficiencies (T) were determined from bilirubin-mediated quenching of AS fluorescence, using equation 8 (51):

$$T = 1 - \left(\frac{I}{I^0}\right) \quad \textit{Eq. 8)}$$

where I and I^0 reflect anthroyloxy probe fluorescence intensity in the presence and absence of bilirubin, respectively. Intensities were integrated between 380 and 700 nm, and scattering background (<0.1%) from unlabeled DOPC vesicles was subtracted. Transfer efficiencies also were determined from the intensity of sensitized emission, according to the method of Kleinfeld (52) (equation 9):

Downloaded from www.jlr.org by guest, on June 14, 2012

$$T = \frac{I_{BR}\varphi_{AS}}{I^{0}_{AS}\varphi_{BR}} \qquad Eq.\ 9)$$

where I_{BR} is the bilirubin fluorescence intensity corrected for direct emission and light scattering (51), I^0_{AS} is the AS fluorescence intensity in the absence of bilirubin, and φ_{AS} and φ_{BR} reflect the fluorescence quantum yield of the AS probe and bilirubin, respectively.

RESULTS

Determination of bilirubin penetration depth, using spin-labeled phospholipids

To determine the depth of penetration of bilirubin into lipid bilayers, we analyzed the quenching of the intrinsic fluorescence of bilirubin by spin-labeled phospholipid probes. For these studies, phosphatidylcholine labeled with a doxyl moiety at either the 5- or 12-position was incorporated into DOPC vesicles at molar ratios ranging from 0% to 75%. Bilirubin was then added to spin-labeled vesicles suspended in 0.1 M potassium phosphate (pH 7.4), and bilirubin steady state fluorescence intensity was recorded (**Fig. 1**, left). When these data are analyzed according to equation 1, the distance from the bilayer center to the bilirubin molecule (z_{cB}) is calculated to be 16.1 ± 1.8 Å (±SD). As the thickness of the hydrocarbon region of the DOPC bilayer hemileaflet is approximately 15 Å (22), these findings support that unconjugated bilirubin localizes to the polar region of the membrane. Identical experiments evaluating the quenching of the fluorescence of BDT by SLPC produced a value for the distance of BDT from the bilayer center (z_{cBDT}) of 15.5 ± 4.5 Å. The hydrophilic mono- and BDT species present in commercial BDT preparations would not be expected to penetrate the membrane bilayer to a significant degree. Thus, the similar localization of unconjugated bilirubin and BDT in the phospholipid bilayer provides additional support for the hypothesis that bilirubin associates near the membrane surface.

Measurement of bilirubin penetration depth in anthroyloxy-labeled vesicles

Unfortunately, in the above-described spin-label experiments, the low fluorescence quantum yield of bilirubin (**Table 1**) results in low signal-to-noise ratios. Moreover, the limited availability of spin-labeled phosphatidylcholines necessitated the use of 12-SLPC. The minimal quenching of bilirubin fluorescence intensity by this probe potentially may result in falsely low calculated values for z_{cB} (24). Therefore, to further validate our depth determinations, an alternative experimental approach was used in which a series of small unilamellar DOPC vesicles containing 1 mol% 2-AS, 6-AS, or 12-AS was prepared and steady state fluorescence was recorded in the presence of increasing concentrations of bilirubin (Fig. 1, right). Studies were conducted at pH 10 because AS probe localizations have been precisely characterized under these conditions (22). Moreover, high pH minimizes the transbilayer flip-flop of AS probes (56) and also reduces the potential for irreversible bilirubin aggregation, which, in the absence of membranes, has been shown to occur at pH values below 8.3 (57). In contrast with experiments using spin-labeled phospholipids, bilirubin quenches the fluorescence intensity of 12-AS to a greater degree than 2-AS, findings that are consistent with *trans* leaflet quenching.

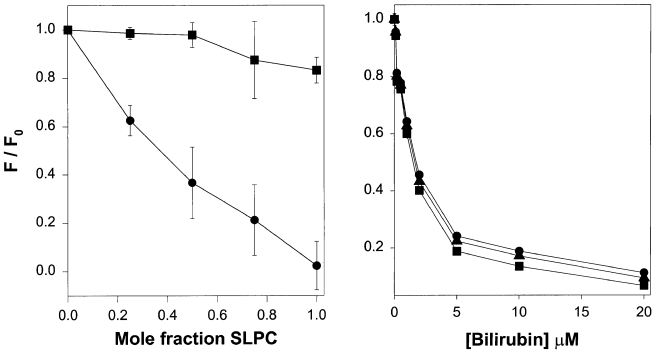

Fig. 1. Measurement of bilirubin penetration depth in DOPC vesicles. Left: Results of studies in which unconjugated bilirubin was added to a suspension of vesicles composed of DOPC and varying concentrations of phosphatidylcholine spin labeled at either the 5-position (circles) or the 12-position (squares). Final concentrations of bilirubin and phospholipid were 2 and 200 μM, respectively. The ratio of bilirubin steady state fluorescence (excitation, 467 nm; emission, 525 nm) in the presence (F) and absence (F_0) of SLPC is plotted against the mole fraction of spin-labeled phospholipid. Each point reflects the mean (±SD) of three experiments conducted at pH 7.4, and is corrected for light-scattering background. By substituting values of 6.3 and 12.15 Å for L_{21} and z_{c1} into equation 1 (22), the distance of bilirubin from the bilayer center is calculated to be 16.1 ± 1.8 Å (±SD). Right: Anthroyloxy stearate probes labeled at either the 2-position (circles), 6-position (triangles), or 12-position (squares) were incorporated into DOPC vesicles at a concentration of 1 mol%. The ratio of the steady state fluorescence (excitation, 360 nm; emission, 490 nm) of a suspension of AS-labeled vesicles (200 μM phospholipid) in the presence (F) or absence (F_0) of unconjugated bilirubin is plotted against the bilirubin concentration. Data reflect the mean ± SD of three experiments performed at pH 10, and are corrected for both bilirubin inner filter effects and light scattering.

TABLE 1. Fluorescence quantum yield and Förster distance values for anthroyloxy stearate probes and unconjugated bilirubin

	2-AS	6-AS	9-AS	12-AS	Bilirubin
Quantum yield (φ)[a]	0.25	0.31	0.32	0.34	0.00087
Förster distance (R_0)[b]	32	34	35	36	

[a] Fluorescence quantum yield (φ) values for unconjugated bilirubin and for 2-, 6-, 9-, and 12-AS in small unilamellar DOPC vesicles at pH 10 were determined relative to quinine sulfate in 0.1 N H_2SO_4 (φ = 0.7). Data obtained from multiple determinations exhibited less than 8% variation, and are consistent with previously reported φ values (39, 51).

[b] R_0 values for AS-bilirubin donor-acceptor pairs in DOPC vesicles were calculated from anthroyloxy stearate fluorescence quantum yields and from bilirubin absorption and AS fluorescence spectra at pH 10 (Fig. 3), using equation 7. Values exhibited <5% variation from multiple determinations and are similar to reported results for AS-heme in egg phosphatidylcholine vesicles (51).

Downloaded from www.jlr.org by guest, on June 14, 2012

The affinity of bilirubin for AS-labeled DOPC vesicles at pH 10 also was determined from the quenching of anthroyloxy fluorescence (**Fig. 2**, top). An association constant (K_a) of 1.67 (±0.03) × 10^6 M^{-1} (±SE) was derived from the slope of a Scatchard plot of the data (Fig. 2, top, inset). Similar results were obtained for BDT (Fig. 2, bottom), with Scatchard analysis indicating a K_a value of 1.63 (±0.04) × 10^6 M^{-1} (±SE) (Fig. 2, bottom, inset). The association of bilirubin with membranes is further evidenced by a shift in the bilirubin absorbance spectrum (**Fig. 3**) and by the marked increase in bilirubin fluorescence yield (Fig. 3, inset) in the presence of added DOPC vesicles.

To permit the determination of membrane penetration depth, it was necessary to measure fluorescence quantum yields (φ) for bilirubin and the various AS probes in DOPC vesicles at pH 10 (Table 1). The measured φ values were then used, in conjunction with the bilirubin absorption spectrum and integrated AS emission spectra (Fig. 3), to calculate Förster distances (equation 7). The relatively large R_0 values with respect to the thickness of the DOPC bilayer highlight the potential for *trans* leaflet quenching of the deeper AS probes by bilirubin. Energy transfer efficiencies for AS-bilirubin donor-acceptor pairs calculated from AS quenching (equation 8) were found to be in close agreement (±10%) with values determined from the sensitized emission (equation 9), indicating that resonance energy transfer is the principal mechanism responsible for bilirubin quenching of AS fluorescence intensity (51). In addition, the highly curved Stern-Volmer plots (**Fig. 4**, left) support the static nature of AS quenching by bilirubin (36, 37). Taken together, these findings validate the use of equations 2 through 4 to determine the membrane localization of bilirubin.

The average distance from the bilayer center to the bilirubin molecule (z_{cB}) was calculated from the quenching of AS probe fluorescence, using equation 4 (**Table 2**). Values for z_{cB} also were determined by plotting the natural log of the ratio of the fluorescence intensity of vesicles containing the shallow (F_1) and deep (F_2) probes versus the bilirubin concentration and fitting the data to equa-

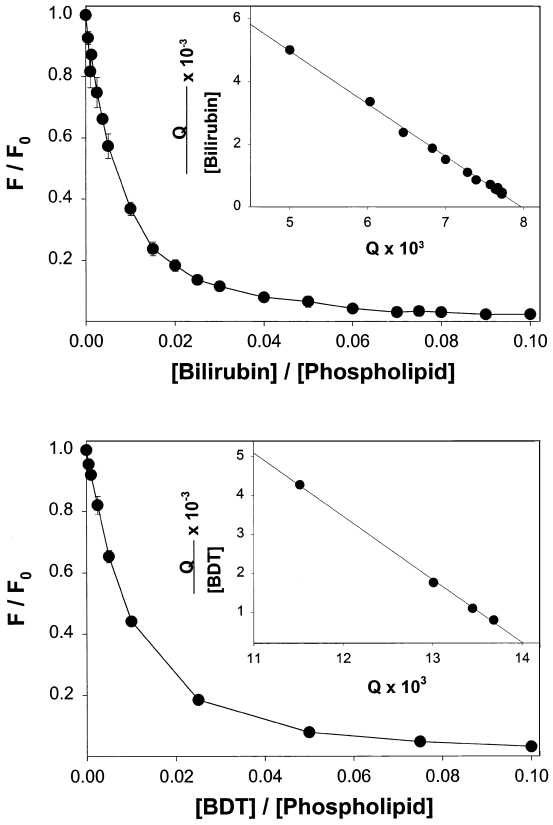

Fig. 2. Bilirubin binding to DOPC vesicles as determined by the quenching of 2-anthroyloxy stearate fluorescence. The affinity of bilirubin (top) and BDT (bottom) for DOPC vesicles (200 μM phospholipid) was determined from the quenching of incorporated 2-anthroyloxy stearate (1 mol%). Data are plotted as the ratio of steady state AS fluorescence (excitation, 360 nm; emission, 490 nm) in the presence (F) or absence (F_0) of bilirubin versus the bilirubin:phospholipid molar ratio. Each point represents the mean ± SD of three experiments conducted at pH 10, and is corrected for the added volume of bilirubin and for inner filter effects. The insets display Scatchard plots of bilirubin (top) and BDT (bottom) binding to 2-AS-labeled DOPC vesicles, where Q reflects the ratio of DOPC-bound bilirubin to total DOPC. Using the method of Levine (40), affinity constants (K_a) of 1.67 (±0.03) × 10^6 M^{-1} and 1.63 (±0.04) × 10^6 M^{-1} (±SE) were calculated from the slope of the linear fits (solid lines, $P < 0.0005$) of the plots for bilirubin and BDT, respectively.

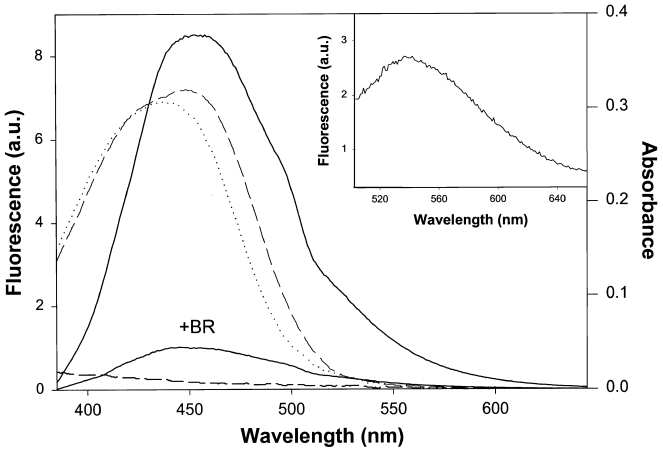

Fig. 3. Fluorescence and absorption spectra in DOPC vesicles. Anthroyloxy fluorescence spectra (solid lines) were obtained by exciting a suspension of small unilamellar DOPC vesicles (200 μM phospholipid) containing 1 mol% 12-AS at 360 nm and pH 10. In the presence of 5 μM bilirubin (+BR), a marked diminution in AS fluorescence intensity, expressed in arbitrary units (a.u.), is observed. The absorption spectrum of bilirubin (6 μM) in the presence (dashed line) or absence (dotted line) of preformed DOPC vesicles (200 μM phospholipid) was obtained at pH 10, using an Amersham Pharmacia (Piscataway, NJ) UltraSpec 2000. The lower dashed line reflects the absorbance spectrum of 12-AS-labeled DOPC vesicles (200 μM phospholipid) in the absence of bilirubin. On the basis of absorbance readings obtained over a range of concentrations, the measured bilirubin extinction coefficient at 440 nm (ε_{440}) in DOPC vesicles is 47,900 M^{-1} cm^{-1}. The inset displays the fluorescence spectrum (excitation, 480 nm) of 5 μM bilirubin in the presence of DOPC vesicles (200 μM phospholipid) at pH 10, after subtracting bilirubin fluorescence intensity in the absence of vesicles.

Downloaded from www.jlr.org by guest, on June 14, 2012

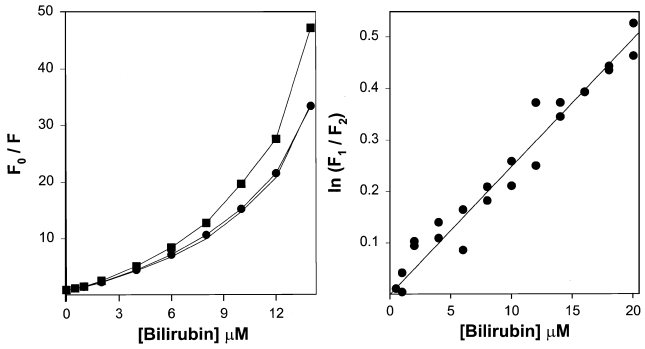

Fig. 4. Quenching of anthroyloxy stearate fluorescence by bilirubin: Stern-Volmer and natural log plots. Left: Ratio of the fluorescence intensity of 2-AS (circles), 6-AS (triangles), or 12-AS (squares) fluorescence (1 mol% in DOPC vesicles), in the absence (F_0) or presence (F) of bilirubin, plotted against the bilirubin concentration. Experimental conditions were identical to those outlined in the right-hand panel of Fig. 1. The highly curved nature of these Stern-Volmer plots suggests that quenching is primarily static (36). Right: A plot of the natural log of the ratio of 2-AS (F_1) to 12-AS (F_2) fluorescence intensity versus bilirubin concentration is displayed. The solid line reflects the best fit of the data to equation 3 ($P < 0.0005$). The linear nature of the plot does not support a concentration-dependent shift in bilirubin localization, which would be expected to manifest as a sharp deviation in slope.

tion 3 (Fig. 4, right). Although values for z_{cB} calculated by these two methods are highly consistent, it is notable that distances calculated from the quenching of the deeper probes (e.g., 9- and 12-AS) are several angstroms farther from the bilayer center as compared with results obtained with the shallower probes. It is notable that all the data presented thus far indicate that bilirubin localizes most closely to the 2- and 6-AS probes. The finding by Abrams and London (24) that depth measurements for AS probes are most accurate when the closest donor-acceptor pair is analyzed suggest that the more precise z_{cB} values are reflected in the quenching of 2- and 6-AS by bilirubin. Therefore, it would appear that the best estimate for the localization of bilirubin is approximately 20 Å from the center of the bilayer, near the membrane-water interface.

TABLE 2. Bilirubin penetration depth as determined by the quenching of anthroyloxy stearate fluorescence[a]

Shallow probe	Deep probe	n	z_{cB} (Å)[b]	z_{cB} (Å)[c]
2-AS	6-AS	3	20.1 ± 0.8	19.6 ± 0.1
2-AS	9-AS	3	23.6 ± 0.7	22.3 ± 0.1
2-AS	12-AS	8	25.1 ± 1.1	25.2 ± 0.8
6-AS	9-AS	3	22.1 ± 0.6	21.9 ± 0.1
6-AS	12-AS	4	24.1 ± 0.9	24.5 ± 0.5
9-AS	12-AS	3	26.1 ± 0.5	25.8 ± 0.9

[a] The distance of bilirubin from the bilayer center (z_{cB}) was determined from the quenching of the fluorescence intensity of DOPC vesicles (200 μM phospholipid) containing 1 mol% of the indicated shallow or deep anthroyloxy stearate probe. All data were obtained at pH 10, with n reflecting the number of sets of experiments performed at each bilirubin concentration (0–20 μM). Distances from the bilayer center to the 2-, 6-, 9-, and 12-AS probes used in the calculations were 16.8, 15.0, 12.6, and 7.5 Å, respectively (24).

[b] Values (± SD) calculated using equation 4.

[c] Values (± SD) derived from the best fit of a plot of the natural log of the ratio of the fluorescence intensity of the shallow and deep probes versus the bilirubin concentration to equation 3. All curve fits were statistically significant ($P < 0.01$).

Effect of the method of bilirubin incorporation on membrane localization

To this point, results have been derived from analyses of the interaction of bilirubin with preformed vesicles. However, other investigators have suggested that the membrane localization of bilirubin may depend on the method of bilirubin incorporation (21). To examine this hypothesis, we determined bilirubin penetration depths in DOPC vesicles in which bilirubin was introduced at the time of vesicle formation. For these studies, vesicles were prepared by sonicating a suspension of appropriate molar ratios of DOPC and bilirubin, in the presence or absence of 2- or 12-AS. Steady state AS fluorescence was recorded and plotted as a function of the concentration of added bilirubin (**Fig. 5**, left). Using this approach we found that, at all concentrations studied, bilirubin quenches 2-AS more effectively than 12-AS, with a calculated z_{cB} of 29.0 ± 0.6 (±SD) obtained with equation 4. This finding supports a more superficial bilirubin localization as compared with measurements obtained in preformed vesicles (Fig. 1, right).

The convex nature of the quenching curve with respect to the concentration of added bilirubin suggests that significant loss of pigment occurs during the process of incorporating bilirubin into vesicles. This conclusion is supported by the marked difference in the absorbance spectrum of samples in which bilirubin is added to preformed DOPC vesicles as compared with when an equivalent quantity of bilirubin is introduced at the time of vesicle preparation (Fig. 5, left, inset). The substantially lower absorbance readings after sonication suggest that the energy introduced by this procedure causes considerable pigment degradation. However, correcting for the loss of pigment by extrapolating bilirubin concentrations from absorbance readings at 440 nm had no significant effect on the calculated penetration depth (z_{cB} = 29.2 ± 0.8). We speculate that the more superficial bilirubin localization in cosonicated vesicles may reflect the presence of water-soluble bilirubin degradation products generated by the sonication procedure.

Iodide quenching of membrane-bound bilirubin

Iodide is an aqueous quencher that interacts with fluorophores present in a polar environment (42). Hence, the ability of potassium iodide to quench the fluorescence of membrane-bound bilirubin versus 2-AS was compared in an attempt to verify the relative localization of these two compounds within the DOPC bilayer. A K_{SV} of 9.6 ± 0.3 M^{-1} (±SE) for bilirubin and 3.3 ± 0.1 M^{-1} for 2-AS were calculated from the slope of the Stern-Volmer plots (Fig. 5, right), on the basis of equation 5. The relatively high K_{SV} for bilirubin is typical of values obtained for exposed tryptophan groups (42, 47), and is consistent with a more superficial localization of bilirubin as compared with 2-AS. Using equation 6, the bimolecular rate constant (k_q) was

Downloaded from www.jlr.org by guest, on June 14, 2012

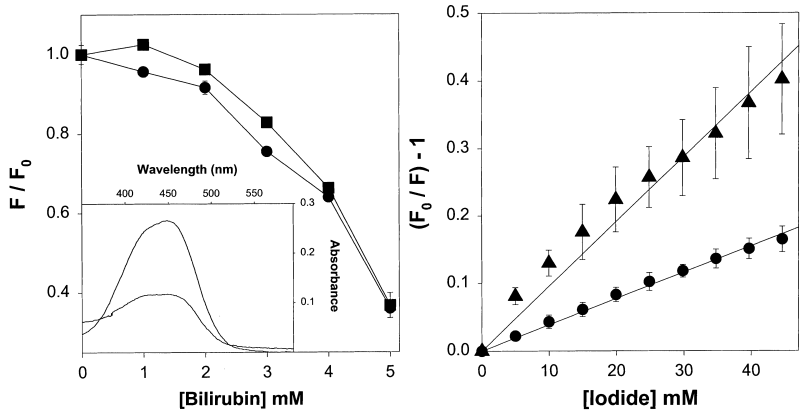

Fig. 5. Localization of bilirubin in cosonicated DOPC vesicles and by iodide quenching. Left: Steady state fluorescence intensity (excitation, 360 nm; emission, 490 nm) of small unilamellar DOPC vesicles (200 μM phospholipid) containing 1 mol% anthroyloxy stearate labeled at the 2-position (circles) or 12-position (squares) in the presence (F) or absence (F_0) of varying concentrations of bilirubin, which was incorporated at the time of vesicle preparation. Data represent the mean (±SD) of three experiments performed at pH 10. The inset displays the absorbance spectrum of 5 μM bilirubin after incorporation into preformed (upper curve) DOPC vesicles (200 μM phospholipid) and immediately after introduction into vesicles by sonication (lower curve). Right: Stern-Volmer plots of the quenching of intrinsic bilirubin (triangles) fluorescence (excitation, 467 nm; emission, 525 nm) and 2-AS (circles) fluorescence (excitation, 360 nm; emission, 490 nm) by potassium iodide are displayed. Bilirubin (5 μM) was incorporated into preformed DOPC vesicles (200 μM), whereas 2-AS (1 mol%) was introduced at the time of vesicle preparation. Points represent the mean (±SD) of three separate experiments, with the solid lines reflecting the best fit of the data to the function $y = mx$ ($P < 0.0005$).

calculated from the measured values for K_{SV} and reported τ_0 values for bilirubin (6 ns) and 2-AS (11.3 ns) (39, 58). The resultant k_q values of 1.6×10^{-9} M^{-1} s^{-1} for bilirubin and 0.3×10^{-9} M^{-1} s^{-1} for 2-AS also are indicative of a shallower penetration depth for the former species. Taken together, these data indicate that DOPC-bound bilirubin is highly accessible to the aqueous environment, and support a localization near the membrane-water interface.

Influence of pH on bilirubin penetration depth

It is notable that the SLPC studies, which indicate a somewhat deeper bilirubin penetration depth as compared with the AS analyses, were conducted at a lower pH (pH 7.4 vs. 10). Hence, we sought to determine the effect of pH on bilirubin penetration depth. On the basis of prior studies demonstrating that the membrane localization of anthroyloxy-labeled fatty acids is modulated by protonation of the carboxyl group (23, 24), we examined the effect of pH on bilirubin penetration depth in DOPC bilayers, anticipating that the uncharged bilirubin diacid would penetrate more deeply than the dianion species (21). Analyses of the quenching of 2- and 12-AS-labeled DOPC vesicles by bilirubin were conducted at both pH 5 and pH 10, as AS probe localization has been precisely defined under these conditions (23).

Unfortunately, we were unable to assess the depth of bilirubin penetration at pH 5 due to limited quenching of anthroyloxy fluorescence (**Fig. 6**, left). For this reason, additional parallax analyses were conducted at physiologic pH. To permit calculation of z_{cB} values at pH 7.4, it was necessary to extrapolate AS probe position. On the basis of previously reported effects of hydrogen ion concentration on AS localization (23), we estimated the distance of the anthroyloxy moiety from the bilayer center at pH 7.4 to be intermediate between that measured at pH 5 and at pH 10. Substitution of these values into equation 4 produced a z_{cB} at pH 7.4 of 22.9 ± 2.0 Å, which is approximately 1 Å lower than the value at pH 10 (24.4 ± 1.1 Å) calculated from the data in Fig. 6. We speculate that the reduced level of AS quenching by bilirubin at higher hydrogen ion concentrations reflects bilirubin aggregation. Self-association of bilirubin monomers in aqueous solution, which previously has been shown to occur (in the absence of phospholipids) at or below pH 10 (59), may be expected to reduce the concentration of bilirubin bound to the phospholipid vesicles, resulting in an underestimation of probe quenching. In this regard, the bilirubin penetration depth calculated from the quenching of bilirubin fluorescence intensity by 5- and 12-SLPC, a technique that is relatively unaffected by the absolute bilirubin concentration, was no different at pH 10 (16.2 ± 3.2 Å) as compared with pH 7.4 (16.1 ± 1.8 Å).

In an attempt to circumvent the potential difficulties encountered with the solubility of unconjugated bilirubin, we examined the effect of pH on the localization of BDT in AS-labeled DOPC vesicles (Fig. 6, right). These results further substantiate the comparable localization of unconjugated bilirubin and BDT within DOPC bilayers, as indicated by the similarity in the slope of the natural log plot of the fluorescence ratio of the shallow and deep probes versus the bilirubin concentration (Fig. 6, right, inset). Analysis of the data by equation 4 suggests that BDT pene-

Downloaded from www.jlr.org by guest, on June 14, 2012

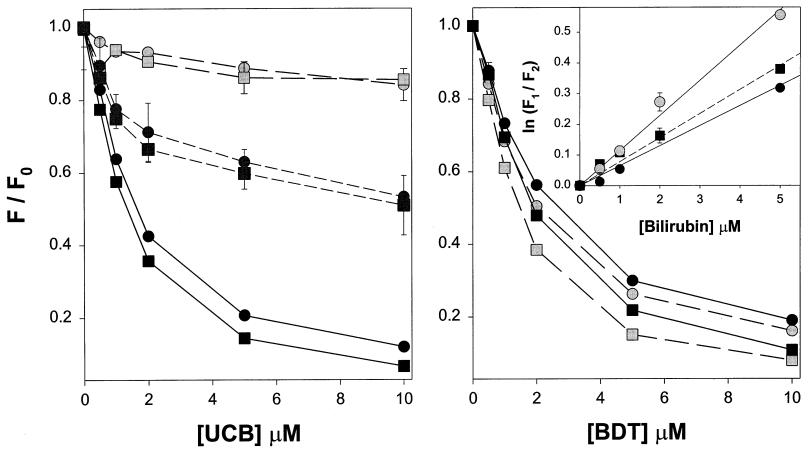

Fig. 6. Effect of pH on the quenching of AS fluorescence intensity by unconjugated bilirubin (UCB) and BDT. Left: Fluorescence intensity of small unilamellar DOPC vesicles (200 μM phospholipid) containing 1 mol% anthroyloxy stearate labeled at the 2-position (circles) or 12-position (squares) was recorded in the presence (F) and absence (F_0) of varying concentrations of UCB. Each point represents the mean (±SD) of three separate experiments conducted at pH 5 (light gray symbols, long dashed lines), pH 7.4 (dark gray symbols, short dashed lines), or pH 10 (solid symbols, solid lines). Extrapolated values for the distance from the bilayer center to the 2- and 12-AS probes used in bilirubin depth calculations were 15.8 and 6.0 Å at pH 5 and 16.3 and 6.8 Å at pH 7.4, respectively (24). Right: Results of identical experiments performed at pH 5 and pH 10, using BDT in place of UCB. In the inset, the fluorescence of anthroyloxy-labeled DOPC vesicles is displayed as the natural log of the ratio of the intensities of 2-AS (F_1) and 12-AS (F_2) fluorescence at pH 5 (gray symbols) and pH 10 (solid symbols). Data (±SD) are plotted against the concentration of BDT (circles, solid line) or UCB (squares, dashed line), with lines reflecting the best fit of the data to equation 3 ($P < 0.0005$). The steeper slope for BDT at pH 5 is indicative of deeper membrane penetration.

trates the bilayer more deeply at pH 5 (z_{cBDT} = 22.7 ± 1.3 Å) as compared with pH 10 (z_{cBDT} = 25.6 ± 1.0 Å). The explanation for the effect of pH on BDT localization is unclear because, extrapolating from the low pK_a values for taurine-conjugated bile acids (60), it is implausible that the difference in penetration depth is the result of changes in the ionization state of the molecule.

Bilirubin localization in small- versus large-diameter vesicles

In the preceding experiments, SUV were utilized to avoid light-scattering effects caused by larger particles. Because of concerns that the inherent lipid-packing constraints of SUV might alter the localization of bilirubin within the bilayer, we determined the effect of vesicle size on bilirubin penetration depth, using a 440-nm cut-on filter to decrease the contribution of light scattering to the fluorescence signal. Both SUV and LUV composed of DOPC and containing 1 mol% 2- or 12-AS were prepared by ethanol injection. The mean hydrodynamic diameters of the SUV and LUV were 35.5 ± 1.0 and 277 ± 15 nm (±SD), respectively, as measured by quasielastic light scattering. On the basis of the quenching of 2- and 12-AS fluorescence (**Fig. 7**), the distance from the bilayer center to the bilirubin molecule was calculated to be 25.9 ± 0.3 Å for SUV, compared with a value of 21.7 ± 1.6 Å for LUV. This difference in bilirubin penetration depth between small- and large-diameter vesicles is consistent with the natural log plots of the ratio of probe fluorescences (Fig. 5, inset). These data suggest that the increased steric constraints inherent to SUV cause the bilirubin molecule to localize several angstroms farther from the bilayer center (61), and are consistent with the findings of prior studies demonstrating a slower rate constant for bilirubin dissociation (33.0 vs. 220 s^{-1}) and higher free energy of activation (15.4 vs. 14.2 kcal mol^{-1}) when bound to LUV versus SUV (17).

Effect of membrane cholesterol content on bilirubin penetration depth

It has been shown previously that the rate of bilirubin solvation from phospholipid vesicles is modulated by membrane cholesterol content (17). Speculating that variations in dissociation rate reflect differences in the depth of bilirubin penetration into the bilayer, we utilized anthroyloxy stearate probes to determine the effect of membrane cholesterol content on the bilirubin localization. DOPC vesicles containing 1 mol% 2- or 12-AS and varying amounts of cholesterol were incubated in the presence of bilirubin at pH 10, and AS steady state fluorescence intensity was recorded. The z_{cB} values calculated from these studies are summarized in **Table 3**. A statistically significant increase in the distance of bilirubin from the bilayer center was observed in vesicles containing the highest concentration of cholesterol (50 mol%), consistent with previous studies demonstrating a faster rate of bilirubin dissociation from vesicles possessing a similar lipid composition (17).

DISCUSSION

In the studies outlined above, we used the technique of fluorescence parallax analysis to determine the depth of

Downloaded from www.jlr.org by guest, on June 14, 2012

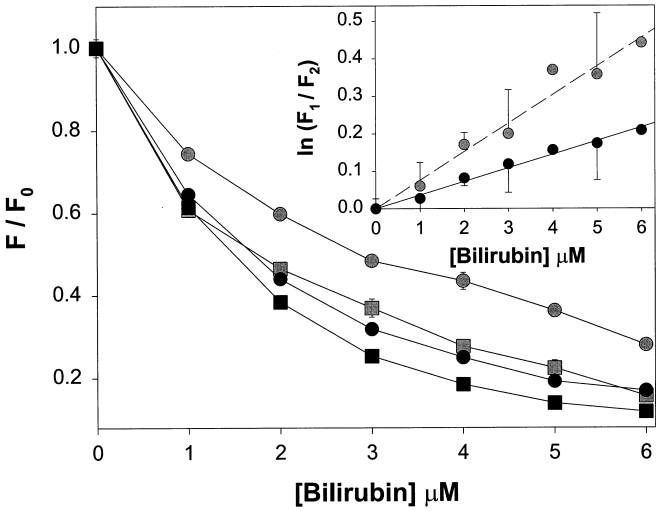

Fig. 7. Influence of vesicle size on bilirubin localization in DOPC vesicles. Anthroyloxy stearate probes labeled at the 2-position (circles) or 12-position (squares) were incorporated into small (solid symbols) or large (gray symbols) unilamellar DOPC vesicles (200 μM phospholipid) at a concentration of 1 mol%. The ratio of AS fluorescence in the presence (F) and absence (F_0) of bilirubin is plotted against the bilirubin concentration. Each point represents the mean ± SD of three experiments conducted at pH 10 and is corrected for bilirubin absorbance. The inset displays a plot of the natural log of the ratio of 2-AS (F_1) to 12-AS (F_2) fluorescence (±SD) versus the bilirubin concentration, with lines reflecting the best fit of the data for small (solid symbols, solid line) and large (gray symbols, dashed line) unilamellar vesicles to equation 3 ($P < 0.0005$).

penetration of bilirubin in model membrane vesicles composed of DOPC. On the basis of the quenching of a series of anthroyloxy stearate probes, we propose that bilirubin localizes to the polar region of small unilamellar vesicles at pH 10, at a distance approximately 20 Å from the bilayer center (**Fig. 8**). This localization is supported by studies of the interaction between membrane-bound bilirubin and potassium iodide, which indicate that bilirubin is more accessible to the aqueous phase than is a 2-AS probe situated 16.8 Å from the center of the bilayer (24). The z_{cB} value extrapolated from the quenching of bilirubin fluorescence by SLPC is 3 to 4 Å smaller than determined with AS probes, although the former studies are constrained by the substantial distance between the bilirubin molecule and 12-SLPC. Despite this discrepancy, the depth measurements derived from each of these distinct methodologic approaches support the conclusion that bilirubin localizes predominantly to the interfacial region of the membrane. This finding is consistent with the dianionic nature of the bilirubin molecule at pH 10, which would not be conducive to penetration of the hydrophobic membrane core.

TABLE 3. Influence of membrane cholesterol content on bilirubin localization

Cholesterol Content (mol%)	z_{cB} (Å)[a]
0	24.7 ± 0.6
10	26.6 ± 1.0
25	25.2 ± 0.4
50	29.7 ± 2.8[b]

[a] The distance of bilirubin from the center of DOPC bilayers (z_{cB}) labeled with 1 mol% 2- or 12-AS, and containing varying molar concentrations of cholesterol, was calculated by equation 4. Each value reflects the mean (±SD) of three separate sets of experiments performed at pH 10 over a range of bilirubin concentrations (0–6 μM). Results were unchanged after correcting for small differences in vesicle diameter resulting from the introduction of cholesterol (17).

[b] $P < 0.05$ versus 0% cholesterol.

Our results are in contradiction with those of Zakim and Wong (10) who, on the basis of the results of high-pressure infrared spectroscopic studies of bilirubin-phospholipid mixtures, suggest that bilirubin intercalates into the polymethylene chain region of lipid bilayers. One possible explanation for these discrepant findings is the potential existence of two distinct populations of membrane-bound bilirubin, as suggested by Cestaro et al. (21). In this regard, Zakim and Wong noted effects of bilirubin on the choline head group of DOPC in addition to changes in the CH_2 symmetric stretching band of the methylene chain segments. Unfortunately, these authors were unable to quantify the relative distribution of bilirubin between the apolar and polar region of the vesicles. However, other studies have shown that low levels of bilirubin (<0.2 mol%) can alter the thermal properties of phosphatidylcholine bilayers (62), suggesting that small amounts of pigment may penetrate the membrane core.

Fluorescence parallax studies potentially may not identify an additional population of bilirubin buried deep within the hydrophobic region of the bilayer, because this technique produces an "average" value for the distance of the subject molecule from the bilayer center (22). Against this possibility is the calculated z_{cB} of 20 Å. Because each DOPC vesicle leaflet is 20 to 22 Å thick (22, 24, 63), even if a second population were present within the bilayer, the vast preponderance of bilirubin molecules must be situated in the polar region of the membrane (assuming that the fluorescence quantum yields of the various bilirubin populations are roughly equivalent). Further evidence against a dual localization is derived from the linear nature of the Stern-Volmer plots for iodide quenching (Fig. 5, right) and from kinetic studies of bilirubin dissociation from phosphatidylcholine vesicles (15, 16), both of which are consistent with a single, homogeneous population of membrane-bound pigment (15, 43).

It is possible that our AS studies were unable to detect a population of bilirubin located deep within the hydrophobic core of the membrane because Förster distances for AS-bilirubin donor-acceptor pairs are relatively large with respect to the thickness of the bilayer. A bilirubin molecule situated in the hydrophobic core region potentially could quench to an equal extent both deep and shallow anthroyloxy probes in the opposite (*trans*) leaflet. As a consequence, fluorescence would cease to be a function of molecule depth (22). However, this situation is pertinent only to AS experiments in which probe fluorescence is quenched by bilirubin, and is not germane to studies in

Downloaded from www.jlr.org by guest, on June 14, 2012

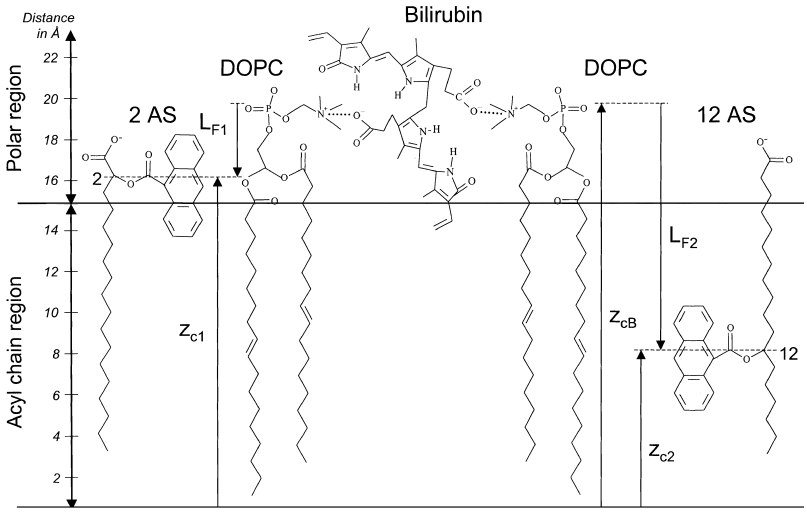

Fig. 8. Schematic illustration of bilirubin localization in a DOPC hemileaflet. Illustrated is the proposed localization of bilirubin in a hemileaflet of dioleoylphosphatidylcholine (DOPC) at a distance ~20 Å from the bilayer center. The polar and apolar regions of the bilayer are identified along the vertical axis, with the distance from the bilayer center represented by tic marks placed at 2-Å increments. Parameters z_{cB}, z_{c1}, and z_{c2} represent the distance from the bilayer center to the bilirubin molecule and to the shallow (2-AS) and deep (12-AS) fluorophores, respectively, while L_{F1} and L_{F2} reflect the distance from the bilirubin molecule to the shallow and deep fluorophores. As has previously been proposed (14), the disruption of internal hydrogen bonding in the bilirubin molecule and the formation of ion pairs (dotted lines) between the bilirubin propionate groups and the quaternary ammonium ions of the choline head group are depicted.

which bilirubin fluorescence is quenched by iodide ions or by SLPC, for which R_c values are on the order of 12 Å (22). Our analyses with spin-labeled probes suggest a somewhat smaller value for z_{cB} as compared with experiments monitoring the quenching of AS, and could be construed as supporting the existence of a relatively small population of bilirubin located deeper within the hydrophobic core. On the basis of our previous data demonstrating that the diacid form of bilirubin is able to spontaneously traverse phospholipid bilayers at pH 7.4 (33), minute levels of this uncharged species are likely to be present within the membrane at physiologic pH.

Cestaro et al. (21) have proposed that the bilirubin dianion binds to the polar head group of phosphatidylcholines whereas the diacid species inserts within the hydrophobic core of the bilayer. We attempted to assess this possibility by conducting parallax analyses under varying pH conditions. Interpretation of these studies is constrained by potentially imprecise estimates of AS probe localization at pH 7.4, and by less substantial fluorescence quenching at lower pH, and we were unable to demonstrate a significant change in the distance of bilirubin from the bilayer center as the pH of the medium was lowered from pH 10 to 7.4. These findings suggest that the charged bilirubin mono- and dianion species that predominate over this range of hydrogen ion concentrations (2, 64) are unlikely to assume a position deep within the hydrophobic core of the membrane. Because bilirubin forms insoluble, metastable colloids at pH values below 8.3 (57), we speculate that the decreased level of AS quenching observed at lower pH (Fig. 6) may reflect irreversible aggregation of bilirubin monomers at the vesicle surface, as has been previously hypothesized (4, 21).

Supporting evidence that bilirubin associates near the membrane surface is provided by resonance Raman spectroscopic analyses of bilirubin-sphingomyelin liposome complexes reported by Yang et al. (14). These studies, which were conducted at pH 9, suggest the formation of an ion pair between the propionate groups of the bilirubin molecule and the quaternary ammonium ion of the choline head group of sphingomyelin (Fig. 8). The bilirubin localization determined by parallax analysis is consistent with the conclusions of these authors. Although it remains uncertain whether the binding of bilirubin to vesicles composed of DOPC accurately reflects the behavior of the molecule in native membranes, support for this contention is derived from the observation that the partitioning of bilirubin into unilamellar DOPC vesicles is similar to that of vesicles composed of plasma membrane lipids (9). The nature of the interaction of bilirubin with cell membranes is particularly relevant to the central nervous system toxicity observed in infants with hyperbilirubinemia, as it is postulated that the neurotoxic effects of bilirubin result from disruption of membrane-based cellular processes (4–6, 65, 66).

These studies were supported by a National Institutes of Health research grant (DK-51679) and a Charles H. Hood Foundation Child Health research award. The authors gratefully acknowledge Dr. Alan Kleinfeld and Dr. Judith Storch for helpful comments, and for their indispensable guidance with experimental design and implementation. The authors also thank Drs. Xiaoyang Qi and Gregory A. Grabowski for assistance with the performance of fluorescence analyses.

Manuscript received 7 April 2000, in revised form 18 January 2001, in re-revised form 9 April 2001, and in re-re-revised form 27 April 2001.

REFERENCES

1. Ostrow, J. D., P. Mukerjee, and C. Tiribelli. 1994. Structure and binding of unconjugated bilirubin: relevance for physiological and pathophysiological function. *J. Lipid Res.* **35:** 1715–1737.
2. Hahm, J. S., J. D. Ostrow, P. Mukerjee, and L. Celic. 1992. Ionization and self-association of unconjugated bilirubin, determined by rapid solvent partition from chloroform, with further studies of bilirubin solubility. *J. Lipid Res.* **33:** 1123–1137.
3. Brodersen, R. 1979. Bilirubin: solubility and interaction with albumin and phospholipid. *J. Biol. Chem.* **254:** 2364–2369.
4. Vazquez, J., M. Garcia-Calvo, F. Valdivieso, and F. Mayor. 1988. Interaction of bilirubin with the synaptosomal plasma membrane. *J. Biol. Chem.* **263:** 1255–1265.
5. Cashore, W. J. 1990. The neurotoxicity of bilirubin. *Clin. Perinatol.* **17:** 437–447.

Downloaded from www.jlr.org by guest, on June 14, 2012

6. Amit, Y., W. Cashore, and D. Schiff. 1992. Studies of bilirubin toxicity at the synaptosome and cellular levels. *Semin. Perinatol.* **16:** 186–190.
7. Talafant, E. 1971. Bile pigment phospholipid interactions. *Biochim. Biophys. Acta.* **231:** 394–398.
8. Tipping, E., B. Ketterer, and L. Christodoulides. 1979. Interactions of small molecules with phospholipid bilayers: binding to egg phosphatidylcholine of some organic anions (bromosulphophthalein, oestrone sulphate, haem and bilirubin) that bind to ligandin and aminoazo-dye-binding protein A. *Biochem. J.* **180:** 327–337.
9. Leonard, M., N. Noy, and D. Zakim. 1989. The interactions of bilirubin with model and biological membranes. *J. Biol. Chem.* **264:** 5648–5652.
10. Zakim, D., and P. T. T. Wong. 1990. A high-pressure, infrared spectroscopic study of the solvation of bilirubin in lipid bilayers. *Biochemistry.* **29:** 2003–2007.
11. Eriksen, E. F., H. Danielsen, and R. Brodersen. 1981. Bilirubin-liposome interaction: binding of bilirubin dianion, protonization, and aggregation of bilirubin acid. *J. Biol. Chem.* **256:** 4269–4274.
12. Brodersen, R. 1982. Physical chemistry of bilirubin: binding to macromolecules and membranes. *In* Bilirubin. K. P. M. Heirwegh and S. B. Brown, editors. CRC Press, Boca Raton, FL. 75–123.
13. Notter, R. H., D. L. Shapiro, R. Taubold, and J. Chen. 1982. Bilirubin interactions with phospholipid components of lung surfactant. *Pediatr. Res.* **16:** 130–136.
14. Yang, B., M. D. Morris, M. Xie, and D. A. Lightner. 1991. Resonance Raman spectroscopy of bilirubins: band assignments and application to bilirubin/lipid complexation. *Biochemistry.* **30:** 688–694.
15. Zucker, S. D., J. Storch, M. L. Zeidel, and J. L. Gollan. 1992. Mechanism of the spontaneous transfer of unconjugated bilirubin between small unilamellar phosphatidylcholine vesicles. *Biochemistry.* **31:** 3184–3192.
16. Noy, N., M. Leonard, and D. Zakim. 1992. The kinetics of interactions of bilirubin with lipid bilayers and with serum albumin. *Biophys. Chem.* **42:** 177–188.
17. Zucker, S. D., W. Goessling, M. L. Zeidel, and J. L. Gollan. 1994. Membrane lipid composition and vesicle size modulate bilirubin intermembrane transfer: evidence for membrane-directed trafficking of bilirubin in the hepatocyte. *J. Biol. Chem.* **269:** 19262–19270.
18. Pownall, H. J., D. L. Hickson, and L. C. Smith. 1983. Transport of biological lipophiles: effect of lipophile structure. *J. Am. Chem. Soc.* **105:** 2440–2445.
19. Massey, J. B., D. H. Bick, and H. J. Pownall. 1997. Spontaneous transfer of monoacyl amphiphiles between lipid and protein surfaces. *Biophys. J.* **72:** 1732–1743.
20. Zhang, F., F. Kamp, and J. A. Hamilton. 1996. Dissociation of long and very long chain fatty acids from phospholipid bilayers. *Biochemistry.* **35:** 16055–16060.
21. Cestaro, B., G. Cervato, S. Ferrari, G. Di Silvestro, D. Monti, and P. Manitto. 1983. Interaction of bilirubin with small unilamellar vesicles of dipalmitoylphosphatidylcholine. *Ital. J. Biochem.* **32:** 318–329.
22. Chattopadhyay, A., and E. London. 1987. Parallax method for direct measurement of membrane penetration depth utilizing fluorescence quenching by spin-labeled phospholipids. *Biochemistry.* **26:** 39–45.
23. Abrams, F. S., A. Chattopadhyay, and E. London. 1992. Determination of the location of fluorescent probes attached to fatty acids using parallax analysis of fluorescence quenching: effect of carboxyl ionization state and environment on depth. *Biochemistry.* **31:** 5322–5327.
24. Abrams, F. S., and E. London. 1993. Extension of the parallax analysis of membrane penetration depth to the polar region of model membranes: use of fluorescence quenching by a spin-label attached to the phospholipid polar headgroup. *Biochemistry.* **32:** 10826–10831.
25. Asuncion-Punzalan, E., and E. London. 1995. Control of the depth of molecules within membranes by polar groups: determination of the location of anthracene-labeled probes in model membranes by parallax analysis of nitroxide-labeled phospholipid induced fluorescence quenching. *Biochemistry.* **34:** 11460–11466.
26. McDonagh, A. F., and F. Assisi. 1972. The ready isomerization of bilirubin IXα in aqueous solution. *Biochem. J.* **129:** 797–800.
27. Abrams, F. S., and E. London. 1992. Calibration of the parallax fluorescence quenching method for determination of membrane penetration depth: refinement and comparison of quenching by spin-labeled and brominated lipids. *Biochemistry.* **31:** 5312–5322.
28. DiCorleto, P. E., and D. B. Zilversmit. 1977. Protein-catalyzed exchange of phosphatidylcholine between sonicated liposomes and multilamellar vesicles. *Biochemistry.* **16:** 2145–2150.
29. Kremer, J. M. H., M. W. J. Esker, C. Pathmamanoharan, and P. H. Wiersema. 1977. Vesicles of variable diameter prepared by a modified injection method. *Biochemistry.* **16:** 3932–3935.
30. Bartlett, G. R. 1959. Phosphorus assay in column chromatography. *J. Biol. Chem.* **234:** 466–468.
31. Cohen, D. E., M. Angelico, and M. C. Carey. 1989. Quasielastic light scattering evidence for vesicular secretion of biliary lipids. *Am. J. Physiol.* **257:** G1–G8.
32. Glushko, V., M. Thaler, and M. Ros. 1982. The fluorescence of bilirubin upon interaction with human erythrocyte ghosts. *Biochim. Biophys. Acta.* **719:** 65–73.
33. Zucker, S. D., W. Goessling, and A. G. Hoppin. 1999. Unconjugated bilirubin exhibits spontaneous diffusion through model lipid bilayers and native hepatocyte membranes. *J. Biol. Chem.* **274:** 10852–10862.
34. Cu, A., G. G. Bellah, and D. A. Lightner. 1975. On the fluorescence of bilirubin. *J. Am. Chem. Soc.* **97:** 2579–2580.
35. Matayoshi, E. D., and A. M. Kleinfeld. 1981. Emission wavelength-dependent decay of the 9-anthroyloxy-fatty acid membrane probes. *Biophys. J.* **35:** 215–235.
36. London, E. 1982. Investigation of membrane structure using fluorescence quenching by spin-labels: a review of recent studies. *Mol. Cell. Biochem.* **45:** 181–188.
37. London, E., and G. W. Feigenson. 1981. Fluorescence quenching in model membranes. 1. Characterization of quenching caused by a spin-labeled phospholipid. *Biochemistry.* **20:** 1932–1938.
38. East, J. M., and A. G. Lee. 1982. Lipid selectivity of the calcium and magnesium ion dependent adenosine triphosphatase, studied with fluorescence quenching by a brominated phospholipid. *Biochemistry.* **21:** 4144–4151.
39. Chen, R. F. 1973. The fluorescence of bilirubin-albumin complexes. *In* Fluorescence Techniques in Cell Biology. A. A. Thaer and M. Sernetz, editors. Springer-Verlag, Berlin. 273–282.
40. Levine, R. L. 1977. Fluorescence-quenching studies of the binding of bilirubin to albumin. *Clin. Chem.* **23:** 2292–2310.
41. Goessling, W., and S. D. Zucker. 2000. Role of apolipoprotein D in the transport of bilirubin in plasma. *Am. J. Physiol.* **279:** G347–G356.
42. Raja, S. M., S. S. Rawat, A. Chattopadhyay, and A. K. Lala. 1999. Localization and environment of tryptophans in soluble and membrane-bound states of a pore-forming toxin from *Staphylococcus aureus. Biophys. J.* **76:** 1469–1479.
43. Nalefski, E. A., and J. J. Falke. 1998. Location of the membrane-docking face on the Ca^{2+}-activated C2 domain of cytosolic phospholipase A_2. *Biochemistry.* **37:** 17642–17650.
44. Wang, Q., D. Cui, and Q. Lin. 1997. Fluorescence studies on the interaction of a synthetic signal peptide and its analog with liposomes. *Biochim. Biophys. Acta.* **1324:** 69–75.
45. Pownall, H. J., and L. C. Smith. 1974. Fluorescence quenching of anthracene in charged micelles. *Biochemistry.* **13:** 2594–2597.
46. Louro, S. R. W., M. Tabak, and O. R. Nascimento. 1994. Depth profiling of dibucaine in sarcoplasmic reticulum vesicles by fluorescence quenching. *Biochim. Biophys. Acta.* **1189:** 243–246.
47. Lehrer, S. S. 1971. Solute perturbation of protein fluorescence: the quenching of the tryptophyl fluorescence of model compounds and of lysozyme by iodide ion. *Biochemistry.* **10:** 3254–3263.
48. Scott, T. G., R. D. Spencer, N. J. Leonard, and G. Weber. 1970. Emission properties of NADH: studies of fluorescence lifetimes and quantum efficiencies of NADH, AcPyADH, and simplified synthetic models. *J. Am. Chem. Soc.* **92:** 687–695.
49. Parker, C. A., and W. T. Rees. 1960. Correction of fluorescence spectra and measurement of fluorescence quantum efficiency. *Analyst.* **85:** 587–600.
50. Birdsall, B., R. W. King, M. R. Wheeler, C. A. Lewis, S. R. Goode, R. B. Dunlap, and G. C. K. Roberts. 1983. Correction for light absorption in fluorescence studies of protein-ligand interactions. *Anal. Biochem.* **132:** 353–361.
51. Kleinfeld, A. M., and M. F. Lukacovic. 1985. Energy-transfer study of cytochrome b_5 using the anthroyloxy fatty acid membrane probes. *Biochemistry.* **24:** 1883–1890.
52. Kleinfeld, A. M. 1988. Tertiary structure of membrane proteins determined by fluorescence resonance energy transfer. *In* Spectroscopic Membrane Probes. L. M. Loew, editor. CRC Press, Boca Raton, FL. 63–92.
53. Dewey, T. G., and G. G. Hammes. 1980. Calculation of fluorescence resonance energy transfer on surfaces. *Biophys. J.* **32:** 1023–1036.

Downloaded from www.jlr.org by guest, on June 14, 2012

54. Trull, F. R., D. P. Shrout, and D. A. Lightner. 1992. Chiral recognition by sulfoxides: induced circular-dichroism from symmetrical mesobilirubin analogs. *Tetrahedron.* **48:** 8189–8198.
55. Kleinfeld, A. M. 1985. Tryptophan imaging of membrane proteins. *Biochemistry.* **24:** 1874–1882.
56. Kamp, F., and J. A. Hamilton. 1992. pH gradients across phospholipid membranes caused by fast flip-flop of un-ionized fatty acids. *Proc. Natl. Acad. Sci. USA.* **89:** 11367–11370.
57. Carey, M. C., and W. Spivak. 1986. Physical chemistry of bile pigments and porphyrins with particular reference to bile. *In* Bile Pigments and Jaundice: Molecular, Metabolic and Medical Aspects. J. D. Ostrow, editor. Marcel Dekker, New York. 81–132.
58. Vincent, M., B. de Foresta, J. Gallay, and A. Alfsen. 1982. Nanosecond fluorescence anisotropy decays of *n*-(9-anthroyloxy) fatty acids in dipalmitoylphosphatidylcholine vesicles with regard to isotropic solvents. *Biochemistry.* **27:** 708–716.
59. Carey, M. C., and A. P. Koretsky. 1979. Self-association of unconjugated bilirubin-IXα in aqueous solution at pH 10.0 and physical-chemical interactions with bile salt monomers and micelles. *Biochem. J.* **179:** 675–689.
60. Cabral, D. J., and D. M. Small. 1989. Physical chemistry of bile. *In* Handbook of Physiology—The Gastrointestinal System. S. G. Schultz, J. G. Forte, and B. B. Rauner, editors. Waverly Press, Baltimore, MD. 621–662.
61. Kachel, K., E. Asuncion-Punzalan, and E. London. 1995. Anchoring of tryptophan and tyrosine analogs at the hydrocarbon-polar boundary in model membrane vesicles: parallax analysis of fluorescence quenching induced by nitroxide-labeled phospholipids. *Biochemistry.* **34:** 15475–15479.
62. Ali, S., and D. Zakim. 1993. The effects of bilirubin on the thermal properties of phosphatidylcholine bilayers. *Biochem. J.* **65:** 101–105.
63. Wiener, M. C., and S. H. White. 1992. Structure of a fluid dioleoylphosphatidylcholine bilayer determined by joint refinement of x-ray and neutron diffraction data. III. Complete structure. *Biophys. J.* **61:** 437–447.
64. Lightner, D. A., D. L. Holmes, and A. F. McDonagh. 1996. On the acid dissociation constants of bilirubin and biliverdin: pK_a values from ^{13}C NMR spectroscopy. *J. Biol. Chem.* **271:** 2397–2405.
65. Ochoa, E. L. M., R. P. Wennberg, Y. An, T. Tandon, T. Takashima, T. Nguyen, and A. Chui. 1993. Interactions of bilirubin with isolated presyntaptic nerve terminals: functional effects on the uptake and release of neurotransmitters. *Cell. Mol. Neurobiol.* **13:** 69–86.
66. Mayor, F., J. Diez-Guerra, and F. Valdivieso. 1986. Effect of bilirubin on the membrane potential of rat brain synaptosomes. *J. Neurochem.* **47:** 363–369.

Downloaded from www.jlr.org by guest, on June 14, 2012